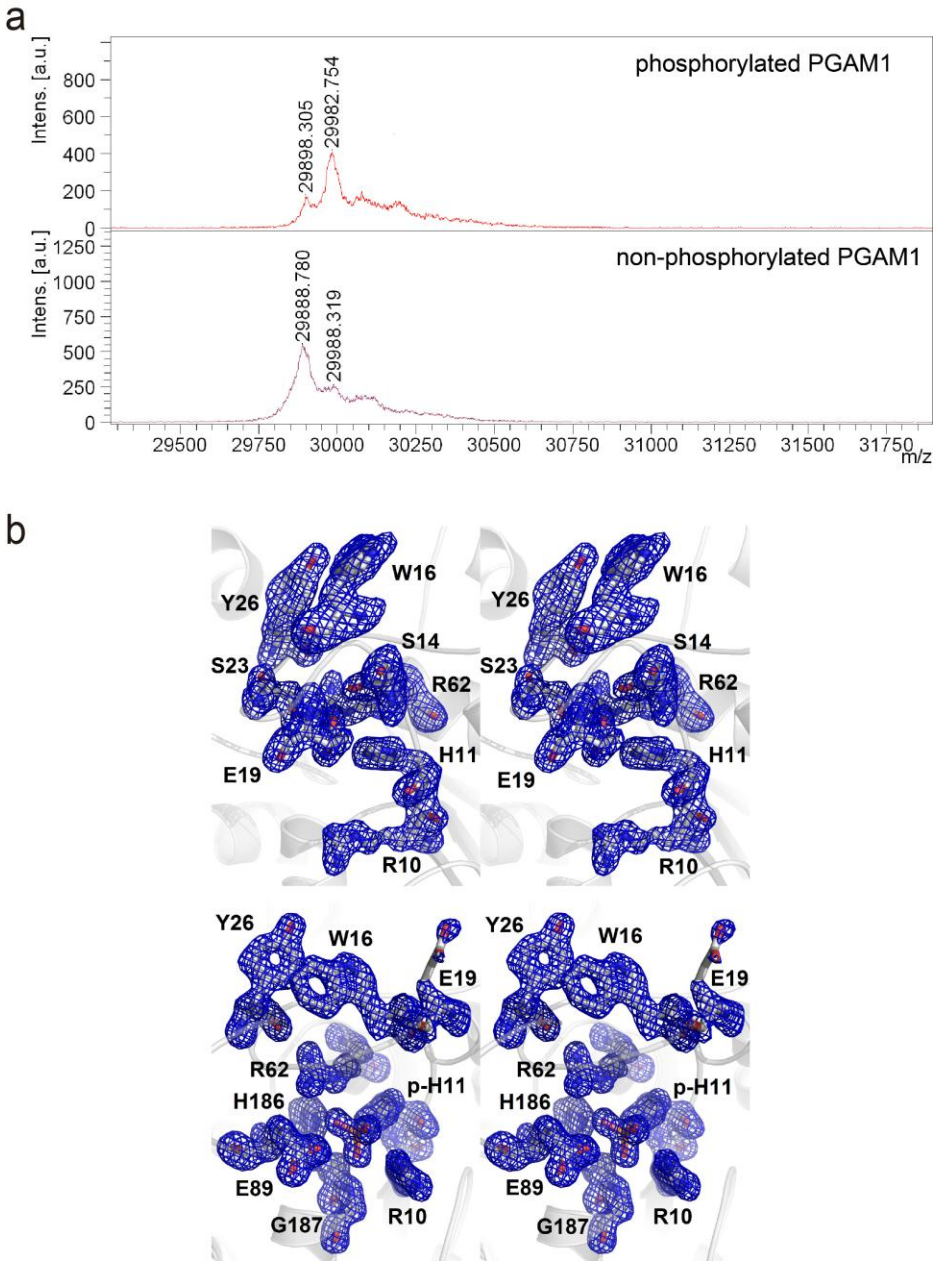

Supplementary Figure S1 | Structural studies of H11-phosphorylated PGAM1. (**a**) Mass spectrum of phosphorylated PGAM1 (top) and non-phosphorylated PGAM1 wild type (bottom). Molecular weight of PGAM1 increased 84 dalton after 2,3-BPG treatment, suggesting that phosphate group (MW: 79) transferred from 2,3-BPG to PGAM1. (**b**) Stereo view of the Fo-Fc electron density map contoured at 3.0 σ around H11. The Fo-Fc density map is shown as blue mesh. Residues of PGAM1 close to H11 are shown in stick. *Upper:* Structure of apo-form PGAM1 in the same orientation as Fig 4c. *Lower:* Structure of H11 phosphorylated PGAM1 in the same orientation as Fig 4d.

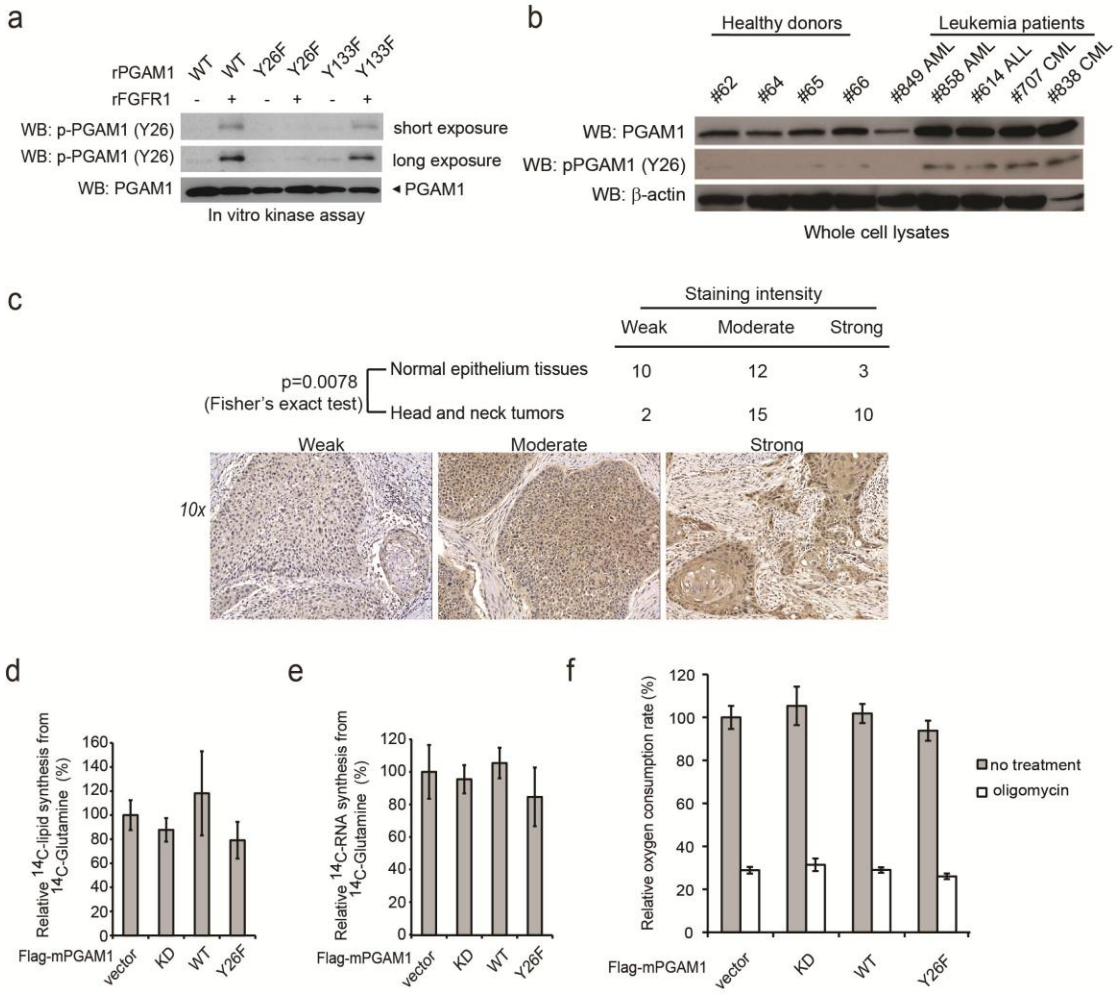

Supplementary Figure S2|Attenuation of PGAM1 does not affect glutamine-dependent biosynthesis of lipids and RNA in H1299 cells. (**a**) Results of Western blot experiment using recombinant PGAM1 protein, including WT, Y26F mutant and control mutant Y133F, treated with purified FGFR1. The phospho-Y26 specific antibody recognises phospho-PGAM1 WT and Y133F but not Y26F. (b) PGAM1 is commonly phosphorylated at Y26 in primary leukemia cells from human patients with CML and AML. BM: bone marrow. PB: peripheral blood. Note that protein expression levels of PGAM1 (top) and □-actin (bottom) in primary leukemia cells from these leukemia patients were previously presented by Hitosugi et al (4; Figure 8C). (**c**) *Upper*: Expression of PGAM1 is significantly upregulated in primary tumor samples of HNSCC patients compared to control normal tissue samples. *Lower*: Representative pictures showing PGAM1 expression assessed by the IHC signal intensity (brown color). (**d-f**) Knockdown of PGAM1 or expression of Y26F mutant in H1299 cells do not affect g lutamine-dependent biosynthesis of lipids (**d**) and RNA (**e**), nor O_2 consumption rate in the presence or absence of 100nM oligomycin (**f**).

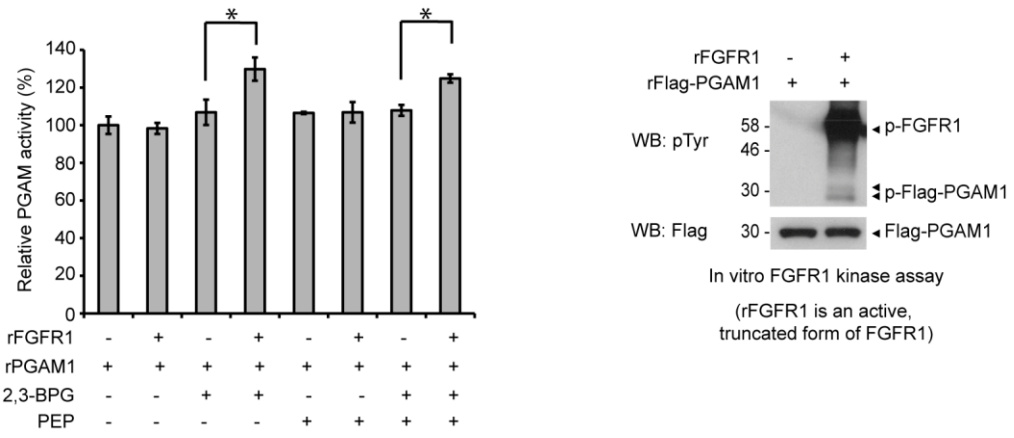

Supplementary Figure S3|Treatment with PEP does not affect the enhanced PGAM1 activation by FGFR1. *Left*: PGAM1 activity was enhanced by treatment with rFGFR1 in the presence or absence of PEP (30μM). *Right*: Control immunoblotting demonstrates tyrosine phosphorylation of recombinant Flag-tagged PAGM1 (rFlag-PGAM1) proteins treated with rFGFR1.

Supplementary Table S1 | Data collection and model statistics of PGAM1 apo-form and H11 phosphorylated-PGAM1.

	PGAM1-apo	phosphorylated-PGAM1
Data Collection		
Space group	$P2_12_12_1$	$P2_12_12_1$
Cell dimensions		
a, *b*, *c* (Å)	81.66, 80.26, 89.28	77.36, 81.17, 90.38
α, β, γ (°)	90.00 90.00 90.00	90.00 90.00 90.00
Resolution* (Å)	30-2.08 (2.15-2.08)	50-1.65 (1.71-1.65)
Completeness (%)	100 (100)	100 (100)
R_{merge}	0.114 (0.988)	0.064 (0.808)
$I/\sigma I$	17.9 (2.1)	26.3 (2.2)
Redundancy	7.2 (7.0)	6.4 (6.2)
Refinement		
Resolution* (Å)	28.6-2.08 (2.11-2.08)	20.0-1.65 (1.67-1.65)
No. reflections	67834	69082
R_{work}/R_{free}	19.4 (23.9)	18.5 (21.4)
No. atoms		
Protein	3833	3863
Ligand/ion	1	12
Water	310	386
B-factor	Protein : 36.7 Solvent: 39.4	
Protein	36.7	27.4
Ligand/ion	21.1	42.7
Water	39.4	37.6
R.m.s. deviations		
Bond lengths (Å)	0.008	0.025
Bond angles (°)	1.069	2.471
Cruickshanks DPI for coordinate error (Å)	0.1430	0.0921
PDB accession code	4GPI	4GPZ

* Highest resolution shell is shown in parentheses.

Supplementary Methods

Reagents. Tyrosine kinase inhibitor (TKI258) was obtained from Novartis Pharma. ShRNA construct for PGAM1 knockdown was purchased from Open Biosystems, Huntsville, AL. The sequence of shRNA used for knockdown is as follows: 5'-CCGGCAAGAACTTGAAGCCTATCAACTCGAGTTGATAGGCTTCAAGTTCTTGTTTTTTG-3'. Murine PGAM1 was flag-tagged by PCR and subcloned into pMSCV-neo

derived Gateway destination vector as described previously [23]. For GST-tagged PGAM1 expression in mammalian cells, PGAM1 variants were subcloned into pDEST27 vector (Invitrogen, Carlsbad, CA). For His-tagged PGAM1 expression in bacterial cells, PGAM1 was subcloned into pET53 vector (Novagen). Phenylalanine mutations (Y26F, Y92F, and Y133F) were introduced into PGAM1 by using QuikChange-XL site-directed mutagenesis kit (Stratagene, La Jolla, CA).

Cell culture. Human cancer cell lines H1299, A549, MDA-MB134, MDA-MB231, HEL, KG1a, Mo91, Molm14, K562, KMS11, and OPM1 were cultured in RPMI 1640 medium with 10% fetal bovine serum (FBS). 293T and MCF7 cells were cultured in Dulbecco Modified Eagle Medium (DMEM) with 10% FBS. LNCaP and 22RV cells were cultured in RPMI 1640 medium with 10% FBS, 1 mM sodium pyruvate, and 10 mM Hepes. 212LN and Tu212 cells were cultured in DMEM/F12 medium with 10% FBS.

Antibodies. Mouse phospho-Tyr antibody pY99, rabbit FGFR1 antibody, rabbit FLT3 antibody were from Santa Cruz Biotechnology, Santa Cruz, CA; rabbit PGAM1 antibody was from Novus; mouse antibodies against GST, Flag and β-actin were from Sigma, St. Louis, MO; rabbit phospho-Jak2 antibody is from CST. Specific rabbit antibody against phospho-PGAM1 (p-Y26) was generated by CST.

In vitro kinase assays. For FGFR1 kinase assay, 200 ng of purified recombinant PGAM1 WT, Y26F and Y133F proteins were incubated with 250 ng of recombinant active FGFR1 (Invitrogen) in FGFR1 kinase buffer [10 mM Hepes (pH 7.5), 150 mM NaCl, 5 mM DTT, 0.01% Triton X-100, 10 mM $MnCl_2$ and 800 μM ATP] for 1 h at 30 °C. For FLT3 kinase assay, 200 ng of purified recombinant PGAM1 WT and Y26F proteins were incubated with 200 ng of recombinant active FLT3 (Invitrogen) in FLT3 kinase buffer [50 mM Hepes (pH 7.5), 2.5 mM DTT, 0.01% NP-40, 10 mM $MgCl_2$ and 200 μM ATP] for 1 h at 30 °C. For Jak2 kinase assay, 200 ng of purified recombinant PGAM1 WT and Y26F proteins were incubated with 200 ng of recombinant active Jak2 (Invitrogen) in Jak2 kinase buffer [25 mM Hepes (pH 7.5), 0.5 mM EGTA, 2.5 mM DTT, 0.01% Triton X-100, 10 mM $MgCl_2$, 0.5 mM Sodium orthovanadate, 5 mM β-glycerophosphate, and 200 μM ATP] for 1 h at 30 °C. For EGFR kinase assay, 200 ng of purified recombinant PGAM1 WT and Y26F proteins were incubated with 200 ng of recombinant active EGFR (Invitrogen) in EGFR kinase buffer [60 mM Hepes (pH 7.5), 1.25 mM DTT, 5 mM $MgCl_2$, 5 mM $MnCl_2$, 3 μM Sodium orthovanadate, and 200 μM ATP] for 1 h at 30 °C.

Glycolytic rate assay. Glycolytic rate was measured by monitoring the conversion of 5-^{3}H-glucose to ^3H_2O. 106 cells were washed once in PBS prior to incubation in 1 ml of Krebs buffer without glucose for 30 min at 37°C. The Krebs buffer was then replaced with Krebs buffer containing 10 mM glucose spiked with 10 μCi of 5-^{3}H-glucose. Following incubation for 1 h at 37°C, triplicate 50 μl aliquots were transferred to uncapped PCR tubes containing 50 μl of 0.2 N HCl, and a tube was transferred into an eppendorf tube containing 0.5 ml of H_2O for diffusion. The tubes were sealed, and diffusion was allowed to proceed for a minimum of 24 h at 34°C. The amounts of diffused ^3H_2O were determined by scintillation counting.

Purification of recombinant PGAM1 proteins. $(His)_6$-tagged PGAM1 proteins were purified by sonication of high expressing BL21(DE3)pLysS cells obtained from 250 mL of culture with IPTG-induction for 4 h. Cell lysates were resolved by centrifugation and loaded onto a Ni-NTA column in 20 mM imidazole. After a step of 2X washing, the protein was eluted with 250 mM imidazole. Proteins were desalted on a PD-10 column and the purification efficiency was examined by coomassie staining and western blotting.

PGAM enzyme assay. PGAM1 activity was measured by multiple enzymes coupled assay. PGAM1 enzyme mix containing 100 mM Tris-HCl, 100 mM KCl, 5 mM $MgCl_2$, 1 mM ADP, 0.2 mM NADH, 5 mg/ml recombinant PGAM1, 0.5 units/ml enolase, 0.5 units/ml recombinant pyruvate kinase M1, and 0.1 units/ml recombinant LDH was prepared. 3-PG was added last at the final concentration of 2 mM to initiate the reaction. The decrease in autofluorescence (ex:340 nm, em:460 nm) from oxidation of NADH was measured as PGAM1 activity.

^{14}C-lipid synthesis assay. ^{14}C-lipids synthesized from ^{14}C-glucose were measured. Subconfluent cells seeded on a 6-well plate were pre-incubated with PGMI-004A for 2 h prior to the addition of ^{14}C-glucose. Cells were then incubated in complete medium spiked with 4 mCi/ml of D-[6-^{14}C]-glucose for 2 h in the presence of PGMI-004A, washed twice with PBS, and lipids extracted by the addition of 500 mL of hexane:isopropanol (3:2 v/v). Well were washed with an additional 500 mL of hexane:isopropanol solution, and all the extracts by the hexane:isopropanol solution were combined and air dried with heat. Extracted lipids were resuspended in 50 mL of chloroform, and subjected to scintillation counting. Scintillation counts were normalised with cell numbers counted by a microscope (x40).

^{14}C-RNA synthesis assay. ^{14}C-RNA synthesized from ^{14}C-glucose was measured. Subconfluent cells seeded on a 6-well plate were pre-incubated with PGMI-004A for 2 h prior to the addition of ^{14}C-glucose. Cells were then incubated in complete medium spiked with 4 mCi/ml of D-[U-^{14}C]-glucose for 2 h in the presence of PGMI-004A. RNA was then extracted using RNeasy columns (Qiagen) and ^{14}C-RNA was assayed by scintillation counter. ^{14}C counts for each sample were normalised by the amount of RNA.

Mass Spectrometry Analysis. Determination of histidine phosphorylation was performed using reversed phase high pressure liquid chromatography-mass spectrometry (HPLC-MS). The immunoprecipitated beads were washed with TBS and Flag-tagged PGAM1 proteins were eluted by 3xFLAG peptide in TBS (Sigma) and directly subjected to MS analysis. PGAM1 WT and Y26F mutant samples were resolved using SDS-PAGE, and PGAM1 containing bands were excised. Bands were digested with trypsin (Promega) overnight at 25°C, and tryptic peptides were extracted with repeated desiccation and swelling in acetonitrile and 100mM ammonium bicarbonate, respectively. The extracted peptides were concentrated by vacuum centrifugation and desalted using in-house made C18STAGE Tips prior to mass spectrometric analysis. Samples were loaded by an Eksigent AS2 autosampler onto a 75 μm fused silica capillary column packed with 11cm of C18 reverse phase resin (5 μm particles, 200Å pore size; Magic C18; Michrom

BioResources). Peptides were resolved on a 110 minute 1-100% buffer B gradient (buffer A = 0.1 mol/l acetic acid, Buffer B = 70% acetonitrile in 0.1 mol/l acetic acid) at a flow rate of 200ml/min (1200 series; Agilent). The HPLC was coupled to a mass spectrometer (LTQ-Orbitrap; ThermoFisher Scientific) with a resolution of 30,000 for full MS followed by seven data-dependent MS/MS analyses. Collision-induced dissociation (CID) was used for peptide fragmentation. Targeted runs were also performed to increase the likelihood of quantifying the labile histidine phosphorylation. Peptide abundance of the phosphorylated and unphosphorylated peptides was calculated by manual chromatographic peak integration of full MS scans using Qual Browser software (version 2.0.7; ThermoFisher Scientific Inc.). The relative abundance of the phosphorylated peptide was calculated as the ratio of the sum of the areas underneath the peaks of phosphorylated peptide to the sum of the areas underneath peaks corresponding to phosphorylated and unphosphorylated peptides (total peptide). The peptide sequence and histidine phosphorylation were confirmed by manual inspection of the MS/MS spectra.

Sample preparation of H11-phosphorylated PGAM1 protein. Purified PGAM1 protein (100 μM, in 20 mM Tris-HCl buffer, pH 7.4) mixed with 2,3-BPG (final concentration: 500 μM) and incubated for half an hour at room temperature. Excess 2,3-BPG was removed by desalting. Purified protein and 2,3-BPG treated protein were directly analyzed by MALDI-TOF mass spectrum using sinapic acid as matrix solution.

Crystallization of PGAM1 proteins and data collection. Crystals of PGAM1 were originally identified using the PEG ION crystallization screen kit (Hampton Research). Optimized crystals were produced using hanging drop vapor diffusion at 16 °C by mixing 1 μL of protein solution at 30-40 mg/mL with 1 μL reservoir solution containing 0.1 M MES pH 6.0, 8% PEG 3350. Crystals appeared after 1 hour and continued to grow for several days. Phosphorylated PGAM1 crystals were obtained by treating wild type PGAM1 with 5 mM 2,3-BPG for half an hour and excess 2,3-BPG were removed by buffer exchange before crystallization. Crystals were dehydrogenated by 50% PEG 6000 for 24 hours, and quickly frozen in liquid nitrogen. All diffraction data were collected at 100K at the macromolecular crystallography for life science beamline LS-CAT (21-ID-F) and NE-CAT (24-ID-C) respectively at the Advanced Photon Source, Argonne National Laboratory. Native data sets extending to 1.65 Å resolution were collected at 0.9795 Å wavelength (12.66 keV). The data were processed with HKL2000 and the scaled data were used for molecular replacement. Crystallographic statistics are summarized in Supplementary Table S1.

Data refinement. For phasing, model building and refinement, the structures of both PGAM1 apo-form and phosphorylated PGAM1 were determined by molecular replacement using Phaser in the CCP4 suite, with the template protein as the search model (pdb code: 1YFK). The structures were then refined by using Phenix. Manual rebuilding of the model was carried out using the molecular graphics program COOT based on electron density interpretation. Water molecules were incorporated into the model if they gave rise to peaks exceeding 3σ in Fo-Fc density maps. The final refined models have good stereochemistry both with 98.5% of the residues in the most favored

regions of the Ramachandran plot with none in the disallowed regions (values calculated using PROCHECK from CCP4 suite).

Cellular metabolites extraction and measurement. Cellular metabolites were extracted and spectrophotometrically measured as described previously (Kauffman et al., 1969; Minakami et al., 1965) with some modifications. To determine cellular concentration of 2-PG and 3-PG, 100 mL of packed cell pellets were homogenized in 1.5 ml of hypotonic lysis buffer (20 mM HEPES (pH 7.0), 5 mM KCl, 1 mM $MgCl_2$, 5 mM DTT, and protease inhibitor cocktail). The homogenates were centrifuged in a cold room at 4^oC for 10 minutes at maximum speed, and the supernatants were applied to Amicon Ultra tubes with 10kDa cut off filter (Millipore). The flow through containing the metabolites was used for the measurement. NADH, ADP, and $MgCl_2$ were added to the flow through to final concentrations of 0.14 mM, 1 mM, and 50 mM, respectively. Recombinant LDH and PKM1 proteins were added to final concentrations of 5 mg/ml and 10 mg/ml, respectively. Recombinant enolase protein was added to a final concentration of 50 mg/ml to measure cellular 2-PG. Once the reaction was initiated by enolase, a decrease in absorbance at 340nm from NADH oxidation was measured by a DU800 spectrophotometer (Beckman). After termination of the enolase reaction, recombinant PGAM1 protein was added to a final concentration of 25 mg/ml and the decrease in absorbance at 340 nm was immediately monitored to measure cellular 3-PG. 100 mL of 2-PG and 3-PG (Sigma) diluted with 1.5 ml of hypotonic lysis buffer were used as the standards.

Oxygen consumption and intracellular ATP assays. Oxygen consumption rates were measured with a Clark type electrode equipped with 782 oxygen meter (Strathkelvin Instruments). 1×10^7 cells were resuspended in RPMI 1640 medium with 10% FBS and placed into a water-jacked chamber RC300 (Strathkelvin Instruments) and recording was started immediately. Intracellular ATP concentration was measured by an ATP bioluminescent somatic cell assay kit (Sigma). 1×10^6 cells were trypsinized and resuspended in ultrapure water. Luminescence was measured with spectrofluometer (SPECTRA Max Gemini; Molecular Probe) immediately after the addition of ATP enzyme mix to cell suspension.

NADPH/$NADP^+$ ratio assay. NADPH/NADP kit (BioAssay Systems) was used to measure cellular NADPH/NADP ratio. Subconfluent cells seeded on a 10 cm dish were collected by a scraper, washed with PBS, and lysed with 200 μL of NADP (or NADPH) extraction buffer. The extract was heated at 60 degree for 5 min and then 20 μL of Assay Buffer and 200 μL of the counter NADPH (or NADP) extraction buffer were added to neutralize the extracts. The extracts were spun down and the supernatants were reacted with working buffer according to the manufacturer's protocol. The absorbance at 565 nm from the reaction mixture was measured with plate reader.

PPP pathway flux assay using $^{14}CO_2$ Release. Cells were seeded on 6-cm dishes placed into a 10-cm dish with 2 sealed holes on the top. $^{14}CO_2$ released from cells was collected by the complete sealing of the 10-cm dish in which the cells on the 6-cm dish were incubated in 2 ml of medium containing [1-^{14}C]- or [6-^{14}C]-glucose, respectively at a

final specific activity of 10 μCi/ml glucose at 37 ^{0}C for 3 h. PPP pathway flux was stopped by injecting 0.3 ml of 2N HCl through the hole on the top, and at the same time $^{14}CO_2$ released was trapped by injecting 0.3 ml of hyamine hydroxide into a small cup placed on the 10-cm dish through another hole. Krebs cycle measurements, obtained in parallel samples incubated with [6-^{14}C]-glucose, were used to correct the PPP pathway flux measurements obtained from samples incubated with [1-^{14}C]-glucose. Each dish was completely re-sealed with parafilms and incubated for O/N at room temperature. Hyamine hydroxide in the small cup was dissolved into 60% methanol and directly subjected to scintillation counting.

Xenograft studies. Nude mice (nu/nu, male 6–8-week-old, Charles River Laboratories) were subcutaneously injected with 10 x 106 H1299 cells stably expressing mPGAM1 WT and Y26F with stable knockdown of endogenous hPGAM1 on the left and right flanks, respectively. Tumour growth was recorded by measurement of two perpendicular diameters of the tumours over a 6-week course using the formula $4\pi/3$ x $(\text{width}/2)^2$ x (length/2). The tumours were harvested and weighed at the experimental endpoint, and the masses of tumours (g) derived from cells expressing mPGAM WT or Y26F mutant in both flanks of each mouse were compared. Statistical analyses have been done by comparison in relation to the control group with a two-tailed paired Student's *t* test.

Primary tissue samples from human patients. Approval of use of human specimens was given by the Institutional Review Board of Emory University School of Medicine. All clinical samples were obtained with informed consent with approval by the Emory University Institutional Review Board. Clinical information for the patients was obtained from the pathological files at Emory University Hospital under the guidelines and with approval from the Institutional Review Board of Emory University School of Medicine and according to the Health Insurance Portability and Accountability Act. Only samples from leukemia patients that were not previously treated with chemotherapy or radiation therapy were used. Mononuclear cells (MNCs) were isolated from peripheral blood samples from human leukemia patients or healthy donors using lymphocyte separation medium (Cellgro). Archived formalin-fixed, paraffin-embedded tumor specimens from HNSSC patients prior to April 2003 were identified from the pathology files in the Department of Pathology and Laboratory Medicine, Emory University Hospital. Clinical information for the patients was obtained from the pathology files in the Department of Pathology patients under the guidelines and approval from the Institutional Review Board of Emory University School of Medicine and according to the Health Insurance Portability and Accountability Act. Only tumors from patients that were not treated previously with either chemotherapy or radiation therapy were used.

Supplementary Reference

23 Chen, J. et al. Constitutively activated FGFR3 mutants signal through PLCgamma-dependent and -independent pathways for hematopoietic transformation. Blood 106, 328-337 (2005).